Chinese Journal of Aeronautics, (2014),27(2): 241–247

Chinese Society of Aeronautics and Astronautics
& Beihang University

Chinese Journal of Aeronautics

cja@buaa.edu.cn
www.sciencedirect.com

Interaction of single-pulse laser energy with bow shock in hypersonic flow

Hong Yanji *, **Wang Diankai, Li Qian, Ye Jifei**

State Key Laboratory of Laser Propulsion & Application, Equipment Academy, Beijing 101416, China

Received 15 April 2013; revised 19 November 2013; accepted 11 December 2013
Available online 19 February 2014

KEYWORDS

Drag;
Flow control;
Navier–Stokes equation;
Shock wave;
Wind tunnel test

Abstract Pressure sensing and schlieren imaging with high resolution and sensitivity are applied to the study of the interaction of single-pulse laser energy with bow shock at Mach 5. An Nd:YAG laser operated at 1.06 μm, 100 mJ pulse energy is used to break down the hypersonic flow in a shock tunnel. Three-dimensional Navier–Stokes equations are solved with an upwind scheme to simulate the interaction. The pressure at the stagnation point on the blunt body is measured and calculated to examine the pressure variation during the interaction. Schlieren imaging is used in conjunction with the calculated density gradients to examine the process of the interaction. The results show that the experimental pressure at the stagnation point on the blunt body and schlieren imaging fit well with the simulation. The pressure at the stagnation point on the blunt body will increase when the transmission shock approaches the blunt body and decrease with the formation of the rarefied wave. Bow shock is deformed during the interaction. Quasi-stationary waves are formed by high rate laser energy deposition to control the bow shock. The pressure and temperature at the stagnation point on the blunt body and the wave drag are reduced to 50%, 75% and 81% respectively according to the simulation. Schlieren imaging has provided important information for the investigation of the mechanism of the interaction.

1. Introduction

With the advantages of high speed and high flight altitude, hypersonic vehicles are widely researched. The pressure and heat flux at the stagnation point on the blunt body and wave drag of a hypersonic vehicle are quite high. Flow control is necessary to enhance the performance. Active flow control is a method to remodel the flow field by localized energy deposition. It has been widely explored in the control of the shock waves in supersonic flow to reduce wave drag or protect the aircraft.[1–3] Georgievsky and Levin[4] reviewed the studies of the interaction of a plane shock with a hot region, and discussed the supersonic interaction of a sphere with a three-dimensional finite inhomogeneous region using the Euler equations. Schülein et al.[5] studied the bow shock interaction with pulse-heated air bubbles experimentally and numerically at Mach 2. Vorticity generation initiated by blast-waves was shown significantly. Kogan et al.[6,7] simulated the peak heat flux and wave drag reduction by supplying heat to a free stream to control the bow shock. Mach number of the free

* Corresponding author. Tel.: +86 10 66364489.
E-mail address: hongyanji@vip.sina.com (Y. Hong).

Peer review under responsibility of Editorial Committee of CJA.

Production and hosting by Elsevier

1000-9361
http://dx.doi.org/10.1016/j.cja.2014.02.006

stream was 2–7. Drag decrease up to 9% was observed for the configuration with the heat source placed before the sphere at the distance of 0.5 sphere radii along the symmetry axis. As a kind of directed energy, laser is applied widely in flow control due to its high power density. Adelgren et al.[8–10] deposited single pulsed laser energy into quiescent air, upstream of bow shock and shock interactions in Mach 3.45 flow to investigate the potential value of flow control with laser energy. Peak pressure with the bow shock and type IV interaction were reduced by 40% and 30% respectively by measurements. Hong[11–15] and Kandala et al.[16–19] studied numerically the influence of laser energy deposition on shock interactions, and the results showed that the pressure and temperature distribution of the blunt body could be remarkably changed. Quasi-stationary waves generated by high-rated laser were applied to reduce the supersonic wave drag. Sasoh et al.[20–24] reduced the wave drag of the blunt body in Mach 1.92 flow with 10 kHz repetitive laser pulses.

The characteristics of a hypersonic flow are unique in some aspects. Experimental study of the interaction of laser pulse with bow shock has not been performed in hypersonic flow conditions. This paper has the purpose to investigate the process of the interaction of single-pulse laser energy with bow shock in Mach 5 flow. The mechanism of the pressure and heat flux at the stagnation point on the blunt body and the wave drag reduction by the interaction is disclosed. The interaction of quasi-stationary waves generated by high-rated laser with hypersonic bow shock is studied.

2. Experimental setup

The experimental setup is shown in Fig. 1. The experiment was performed in a shock tunnel at Mach 5. The experiment time of the shock tunnel was about 10 ms. The diameter of the test section was 100 mm. Helium was selected as the drive gas with $p_4 = 1.5$ MPa. Air was the driven gas with $p_1 = 0.25$ MPa, where p_4 and p_1 are the pressure of drive and driven sections respectively. The diameter of the blunt body was 20 mm. Two PCB sensors were set at the driven section to detect the speed of the incident and the reflected shock waves, which were applied to confirm the total pressure and temperature of the shock tunnel. Total pressure p_5 and temperature T_5 were 2.3 MPa and 600 K respectively. The calculation equation according to shock tube theory is:

$$\frac{p_5}{p_1} = \frac{\left[2r_1 Ma_s^2 - (r_1 - 1)\right]\left[(3r_1 - 1)Ma_s^2 - 2(r_1 - 1)\right]}{(r_1 + 1)\left[(r_1 - 1)Ma_s^2 + 2\right]} \quad (1)$$

$$\frac{T_5}{T_1} = \frac{\left[2(r_1 - 1)Ma_s^2 - (r_1 - 3)\right]\left[(3r_1 - 1)Ma_s^2 - 2(r_1 - 1)\right]}{(r_1 + 1)^2 Ma_s^2} \quad (2)$$

where Ma_s is the Mach number of the incident shock wave detected by the two PCB sensors; $\gamma_1 = 1.4$ is the specific heat ratio of the driven section; T_1 is the temperature of the driven section.

Diagnostic technology with high resolution and sensitivity was required in this study due to the high speed and low density of the hypersonic flow. Schlieren imaging was used in this paper to display the flow field. The main difficulties and corresponding solutions are described as follows: (a) The magnitude of the exposure should be great to capture the details of the interaction, which required a high level brightness of the light source. A flash xenon lamp illuminated by high voltage breakdown xenon was used to solve this problem. (b) The process of the interaction was fast, which requires a high frequency of camera recording. A high speed ICCD camera (PCO-HSFC) with 1280×1024 pixels resolution was used. Exposure time could be as short as 3 ns. Four channels worked independently. (c) The blast wave induced by laser energy in the low density flow was weak, which needed high sensitivity of the schlieren imaging system. Slots were used to restrict the light source in a 0.5 mm × 20 mm rectangle to increase the sensitivity. The schlieren imaging system was presented in imaginary line in Fig. 1. Exposure time of the schlieren imaging was 500 ns in this study.

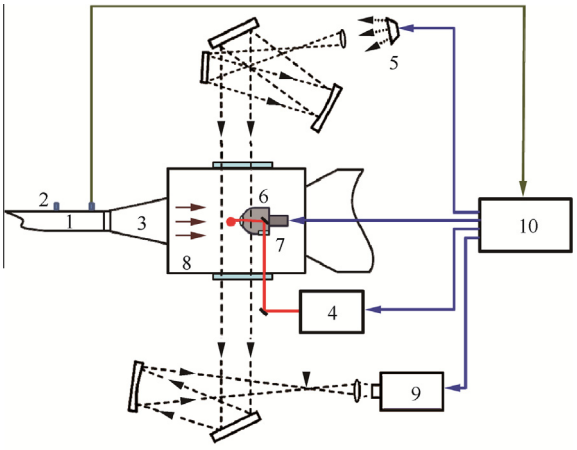

1—Shock tube; 2 and 7—PCB sensor; 3—Laval nozzle at Mach 5;
4—Nd:YAG laser; 5—Flash xenon lamp; 6—Blunt body;
8—Vacuum tank; 9—PCO-HSFC camera; 10—DG645

Fig. 1 Schematics of the experimental setup.

The pressure measurements at the stagnation point on the blunt body were performed with a piezoelectric pressure sensor (PCB-111A24). The sensitivity of the sensor was 0.73 mV/kPa with ±10% error. The sensor was connected through a signal conditioner (PCB-482C16) to a data collector (PCI4712, 40MSs) and then to a computer. The sampling frequency was 10 MHz.

A single-pulse of laser energy was delivered to the flow by an Nd:YAG laser operating at 10.6 μm with a maximum beam power of approximately 600 mJ, which was attenuated to 100 mJ by passing it through the lenses and mirrors. The laser energy was measured by a standard laser energy meter (Laserpoint). The laser light was focused using a convex lens with 150 mm focal length. The distance between the deposition point and the blunt body was 25 mm. The blunt body was two dimensional. Both the diameter and the width were 20 mm.

A digital generator DG645 (Stanford Research System) was employed to supply a preset time sequence for the laser energy, flash xenon lamp, data acquisition of the PCB sensor and high speed camera. Time zero of the DG645 was defined by the incidence shock of the shock tube which was detected by a PCB sensor.

3. Calculation method

Nonstationary compressible three-dimensional Navier–Stokes equations were solved with an upwind scheme to simulate the interaction. The calculation was second order accurate scheme based on the finite volume method and the domain decomposition of the structural grid. An implicit difference method was employed. An upwind scheme based on a rotating Riemann solver was used to calculate the inviscid flux. A perfect gas model was used. The pulse duration of laser was 10 ns in the experiment, which was very short compared with the flow evolution. So laser energy was deposited instantaneously, while the generation and progress of the plasma could be ignored. Laser energy was deposited in the area with a diameter of 2 mm. The equation is:

$$\frac{\partial \boldsymbol{Q}}{\partial t}+\frac{\partial \boldsymbol{F}}{\partial x}+\frac{\partial \boldsymbol{G}}{\partial y}+\frac{\partial \boldsymbol{H}}{\partial z}=\frac{\partial \boldsymbol{F}_{\mathrm{v}}}{\partial x}+\frac{\partial \boldsymbol{G}_{\mathrm{v}}}{\partial y}+\frac{\partial \boldsymbol{H}_{\mathrm{v}}}{\partial z}+\boldsymbol{S} \tag{3}$$

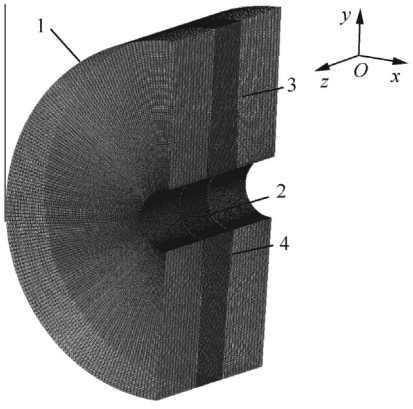

1—Farfield; 2—Wall; 3 and 4—Extrapolate

Fig. 2 Grid and boundary definition.

where $\boldsymbol{Q}$ is the conservation variable, $\boldsymbol{F}$, $\boldsymbol{G}$ and $\boldsymbol{H}$ are the inviscid functions; $\boldsymbol{F}_{\mathrm{v}}$, $\boldsymbol{G}_{\mathrm{v}}$ and $\boldsymbol{H}_{\mathrm{v}}$ are the viscid functions; $\boldsymbol{S}$ is the energy source.

$$\begin{cases} \boldsymbol{Q}=[\rho\ \rho u\ \rho v\ \rho w\ \rho E]^{\mathrm{T}} \\ \boldsymbol{F}=[\rho u\ \rho uu+p\ \rho vu\ \rho wu\ \rho Eu+pu]^{\mathrm{T}} \\ \boldsymbol{G}=[\rho v\ \rho uv\ \rho vv+p\ \rho wv\ \rho Ev+pv]^{\mathrm{T}} \\ \boldsymbol{H}=[\rho w\ \rho uw\ \rho vw\ \rho ww+p\ \rho Ew+pw]^{\mathrm{T}} \end{cases} \tag{4}$$

$$\begin{cases} \boldsymbol{S}=[0\ 0\ \rho\Omega w-\rho\Omega v\ 0]^{\mathrm{T}} \\ \boldsymbol{F}_{\mathrm{v}}=[0\ \tau_{xx}\ \tau_{yx}\ \tau_{zx}\ \beta_x]^{\mathrm{T}} \\ \boldsymbol{G}_{\mathrm{v}}=[0\ \tau_{xy}\ \tau_{yy}\ \tau_{zy}\ \beta_y]^{\mathrm{T}} \\ \boldsymbol{H}_{\mathrm{v}}=[0\ \tau_{xz}\ \tau_{yz}\ \tau_{zz}\ \beta_z]^{\mathrm{T}} \end{cases} \tag{5}$$

where ρ and p are the gas density and pressure, respectively; u, v and w are the velocity components; E is the total energy of gas per unit volume; Ω is the rotary velocity; $\boldsymbol{\tau}$ is the stress; $\boldsymbol{\beta}$ is the energy.

Since the laser pulse duration was 10 ns in the experiment, which was quite short compared with the process of the flow field, laser energy deposition was assumed as an instantaneous deposition. Internal energy increased as the laser energy deposited. The specific internal energy before laser energy deposition is:

$$e_{\mathrm{old}}=E-\frac{1}{2}(u^2+v^2+w^2) \tag{6}$$

The total energy of the laser in the deposition area is:

$$Q_{\mathrm{in}}=\frac{P\Delta t}{\rho V} \tag{7}$$

where V is the volume of the deposition area; P is the power of the laser, and Δt is the duration of the laser pulse.

Assume the laser energy was deposited uniformly. The specific internal energy in each calculation cell after laser deposition was:

$$e=\frac{Q_{\mathrm{in}}}{\rho V}+e_{\mathrm{old}}=\frac{P\Delta t}{\rho V}+E-\frac{1}{2}(u^2+v^2+w^2) \tag{8}$$

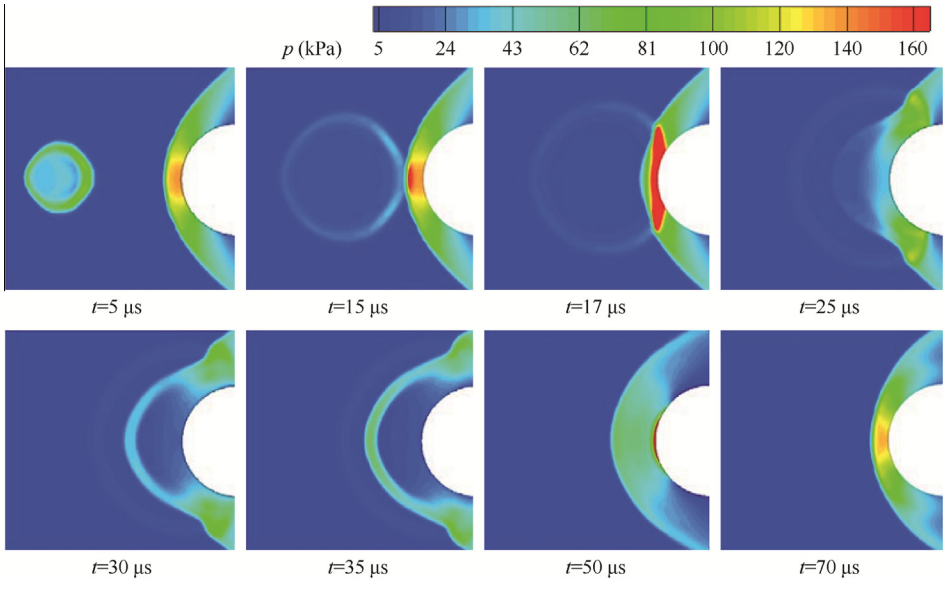

Fig. 3 Distribution of pressure at different times.

In the condition of high rate laser pulse, the function of the laser energy can be described as:

$$f(t) = \begin{cases} Q, \ 0 \leqslant \mathrm{mod}(t, \frac{1}{f}) \leqslant \Delta t \\ 0, \ \Delta t \leqslant \mathrm{mod}(t, \frac{1}{f}) \leqslant \dfrac{1}{f} \end{cases} \tag{9}$$

where Q is the single-pulse laser energy; f is the frequency of the laser pulse. Dual-time stepping methods with an implicit algorithm were adopted to solve the stiff problems caused by the energy terms.

Mach number of the free stream was 5. Static pressure p_∞ and temperature T_∞ were 4349 Pa and 100 K respectively, which were defined according to the experiment. The size of the blunt body was the same as the experiment. The diffraction zone was 30 mm wide at each side of the blunt body. The structural grids were generated with commercial software GridgenV15, and the total number was 90,000. There were about two cells in 1 mm^3 near the wall. No-slip wall conditions were applied on the surface of the blunt body. The grid and definition of the boundary were shown in Fig. 2. The calculation program was developed on our own.

4. Results and discussion

The pressure distributions at different times since the deposition were shown in Fig. 3. Divided by the value without the interaction, both the simulated and the experimental pressure at the stagnation point on the blunt body were normalized in Fig. 4. In Fig. 4, θ is the angle of the blunt body surface. The interaction of a single pulsed laser energy with the bow shock could be described in three steps.

Step 1: From laser energy depositing to t = 15 μs. The laser induced blast wave expanded while moving towards the blunt body with the incoming flow. The peak pressure and temperature of the blunt body was about 1.4×10^5 Pa and 600 K. The distribution had not been changed significantly.

Step 2: The laser induced blast wave interacted with the bow shock. The flow was compressed by the transmission shock wave. At t = 15 μs the blast wave interacted with the bow shock and generated a transmission shock. A local high pressure region was generated. At t = 17 μs, the transmission shock wave approached the blunt body, causing the first peak value of the pressure at the stagnation point on the blunt body. The experimental result was 2.6×10^5 Pa, while the simulated result was 4.3×10^5 Pa. The cause of the difference lay in the perfect gas model in the simulation. Molecular ionization was ignored, so the calculated pressure would be higher. The transmission shock wave transmitted downstream and a rarefied wave was formed near 0°, so the pressure at the stagnation point on the blunt body decreased acutely. At other angles, the transmission shock transmitted downstream along the blunt body, causing local pressure and temperature to increase. At t = 35 μs, the high pressure region was detached from the blunt body, and the pressure at the stagnation point on the blunt body was as low as 5 kPa. The second peak at t = 45 μs and valley at t = 53 μs were caused by the interaction of the upstream portion of the laser energy deposition blast wave and the bow shock. This interaction was not so intensive as the foregoing one, so the pressure changed less markedly.

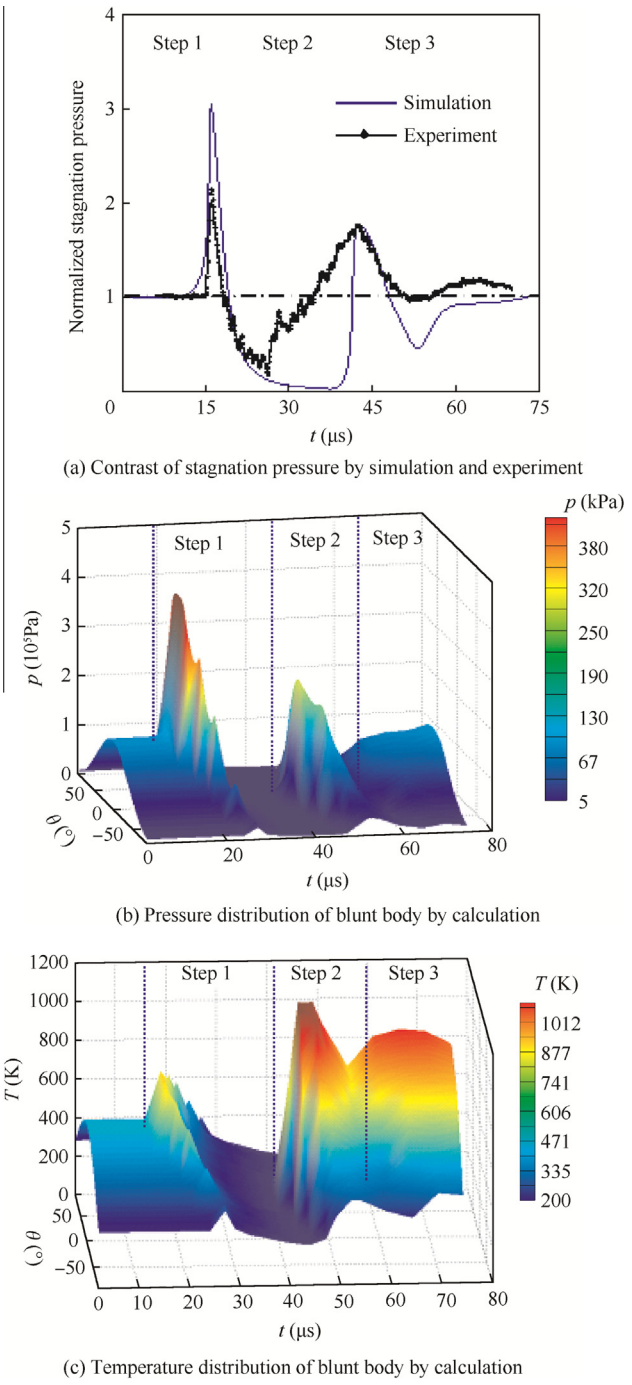

Fig. 4 Pressure and temperature at stagnation point on the blunt body.

Step 3: With the effect of the laser energy coming to an end, the flow field recovered to the initial condition. The temperature at t = 70 μs was about two times that of the initial value while the pressure was about the same, which meant the high temperature was not caused by the shock wave. The cause was that the higher temperature level accu-

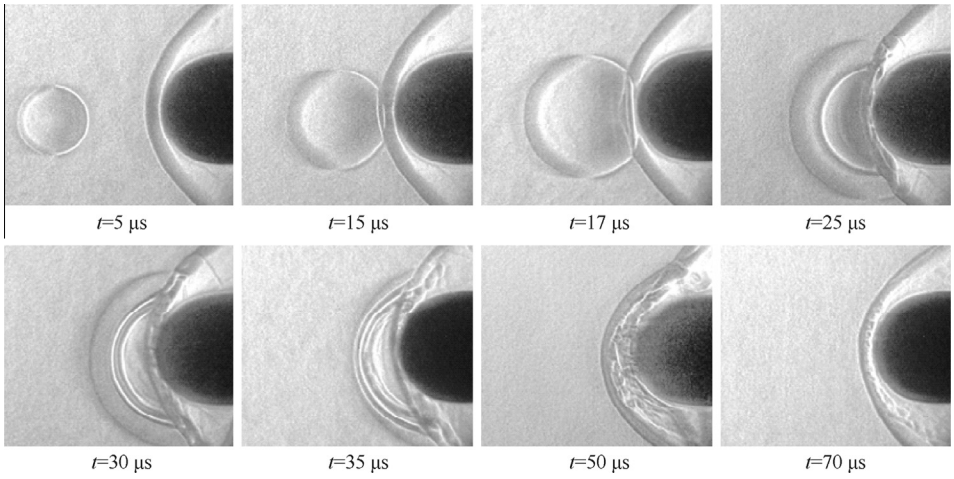

Fig. 5 Schlieren images.

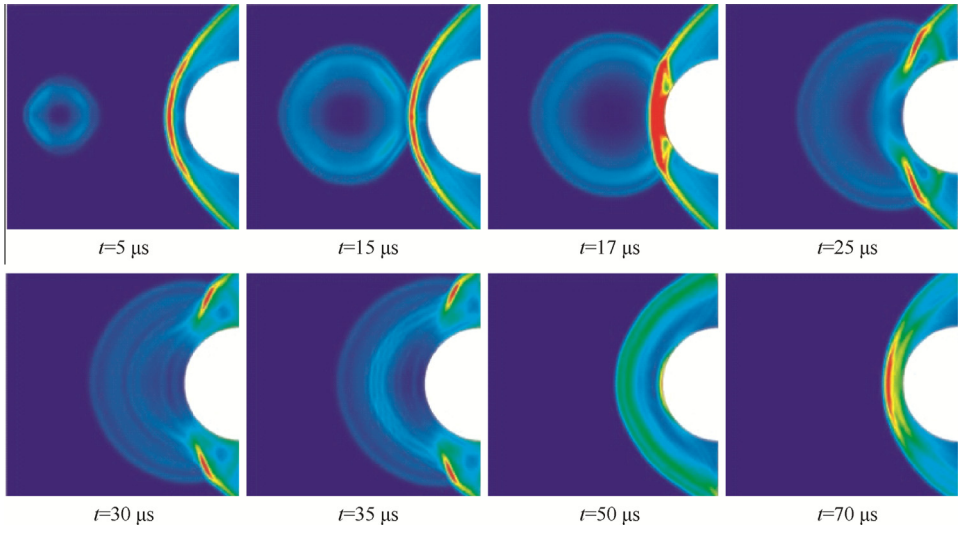

Fig. 6 Calculated density gradients integrated along z axis.

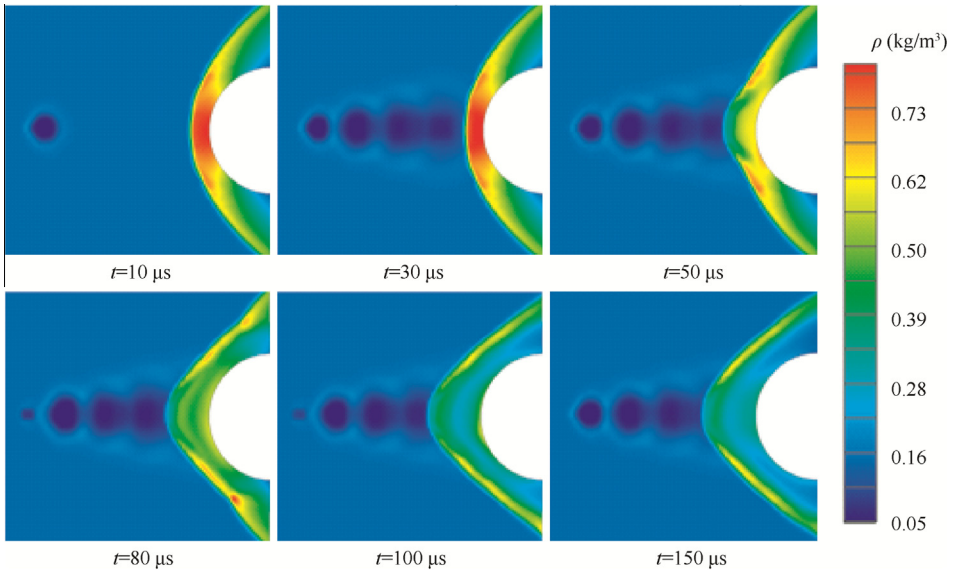

Fig. 7 Process of the flow field with high rate laser pulses.

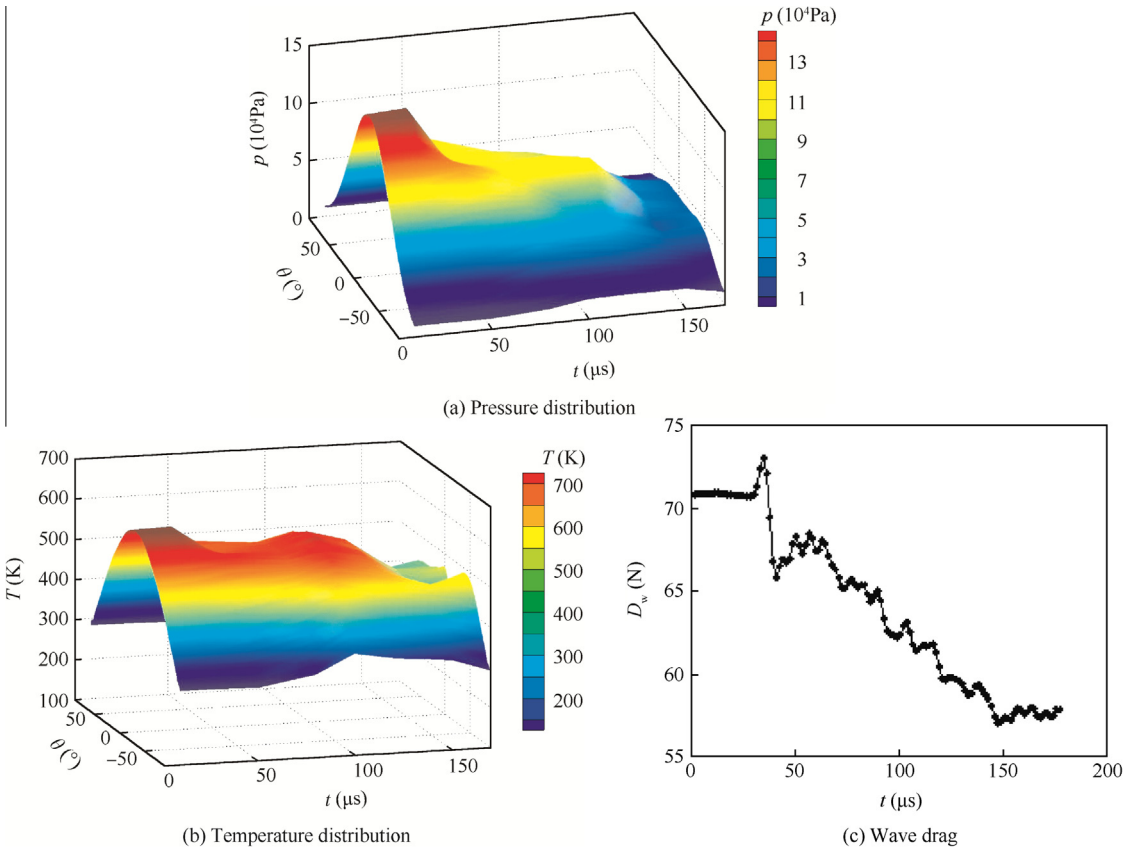

Fig. 8 Variation of the parameters with high rate laser deposition.

mulated in the heated air bubble by laser energy deposition reached the blunt body. Turbulence caused by heat was shown in schlieren images in Fig. 5.

To further disclose the mechanisms of the interaction of laser energy with bow shock, the shock wave structures were studied. Fig. 5 was the schlieren images. Fig. 6 was the calculated density gradients integrated along z axis. The calculated shock structures fitted well with the experiment. Laser induced blast wave and transmission shock were clear both in calculation and experiment. With a rarefied wave formed at the stagnation point, the low pressure region was formed near the stagnation point. Transmission shock moved downstream along the blunt body. The bow shock was deformed due to the interaction during $t = 25$ μs to $t = 50$ μs, which was the so called lens effect. The left half of the blast wave, the deformed bow shock and the reflected blast wave were combined together. Turbulence appeared at $t = 50$ μs due to the heat transfer.

The duration of the low pressure region caused by lens effect was quite short in the case of a single pulse. The pressure and temperature at the stagnation point on the blunt body increased sharply after the lens effect. Consequently, high rate laser energy was considered. In calculation, 150 kHz frequency laser was deposited 20 mm upstream of the blunt body with a pulsed energy of 5 mJ. So the total deposited energy during 80 μs was 60 mJ, which was 0.6 times that of the single pulsed condition. But the pressure and the wave drag reduced by 50% and 19% respectively, which meant the high rate laser was much more efficient. The process of the flow field after the laser deposition was seen in Fig. 7. At $t = 10$ μs, one blast wave was generated with the first pulse. At $t = 30$ μs, four blast waves had been generated and combined as a quasi-stationary wave. Since $t = 50$ μs, the quasi-stationary wave interacted with the bow shock and the bow shock was deformed upstream. The off-body distance between the bow shock and the blunt body was enlarged. The pressure and temperature at the stagnation point on the blunt body and wave drag D_w were reduced significantly, as shown in Fig. 8.

5. Conclusions

(1) High resolution schlieren technique was developed and three-dimensional Navier–Stokes equations were solved to study the interaction of single-pulse laser energy with bow shock in a Mach 5 flow. The process of the interaction was clearly presented. The results indicate that: the bow shock was deformed during the interaction, a rarefied wave was formed near the stagnation point at the same time, causing a low pressure region. The calculated peak pressure was much higher than the experiment due to the perfect gas model.

(2) The low pressure region during $t = 25$ μs to $t = 35$ μs suggested that laser energy deposition would be a potential method to reduce the pressure at the stagnation point on the blunt body and wave drag. To maintain

the low pressure region, high rate laser energy at 150 kHz was deposited to control the bow shock. A quasi-stationary wave was formed after four pulses. The pressure and temperature at the stagnation point on the blunt body and wave drag were reduced to 50%, 75% and 81% respectively.

(3) Mach number in this study was 5, which was much higher than the previous studies. The schlieren images were quite clear. Details of the hypersonic interaction of pulse-heated air bubble were formulated. The mechanisms of hypersonic wave drag reduced by the quasi-stationary wave generated with high rate laser energy were disclosed. The quasi-stationary wave showed a potential application in wave drag reduction. High temperature gas models should be considered in further study.

Acknowledgement

This study was supported by the National Natural Science Foundation of China (No. 11372356).

References

1. Bletzinger P, Ganguly BN, Van Wie D, Garscadden A. Plasmas in high speed aerodynamics. *J Phys. D: Appl Phys* 2005;**38**(4):33–57.
2. Tret'yakov PK, Garanin AF, Grachev GN, Krainev VL, Ponomarenko AG, Tishchenko VN, et al. Control of supersonic flow around bodies by means of high-power recurrent optical breakdown. *Phys-Dokl* 1996;**41**(11):566–7.
3. Knight D, Kuchinskiy V, Kuranov A, Sheikin E. Survey of aerodynamic flow control at high speed by energy deposition. In: *Proceedings of 41st aerospace sciences meeting and exhibit*; 2003 Jan 6–9; Reno, Nevada. Reston, VA: AIAA; 2003.
4. Georgievsky PY, Levin VA. Unsteady Interaction of a sphere with atmospheric temperature inhomogeneity at supersonic speed. *Fluid Dyn* 1993;**28**(4):568–74.
5. Schülein E, Zheltovodov AA, Pimonov EA, Loginov MS. Experimental and numerical modeling of the bow shock interaction with pulse-heated air bubbles. *Int J Aerosp Innovations* 2010;**2**(3):165–87.
6. Kogan MN, Starodubtsev MA. Reduction of peak heat fluxes by supplying heat to the free stream. *Fluid Dyn* 2003;**38**(1):115–25.
7. Kogan MN, Ivanov DV, Shapiro EL, Yegorov IV. Local heat supply influence on a flow over a sphere. In: *Proceedings of 38th aerospace sciences meeting & exhibit*; 2000 Jan 10–13; Reno, Nevada. Reston, VA: AIAA; 2000.
8. Adelgren RG, Elliott GS, Knight D, Zheltovodov A, Beutner TJ. Energy deposition in supersonic flows. In: *Proceedings of 39th AIAA aerospace sciences meeting & exhibit*; 2001 Jan 8–10; Reno, Nevada. Reston, VA: AIAA; 2001.
9. Adelgren RG, Hong YG, Elliott GS, Beutner TJ, Zheltovodov A, Ivanov M. Localized flow control by laser energy deposition applied to edney IV shock impingement and intersecting shocks. In: *Proceedings of 41st aerospace sciences meeting and exhibit*; 2003 Jan 6–9; Reno, Nevada. Reston, VA: AIAA; 2003.
10. Adelgren RG. Localized flow control with energy deposition. Final report. WPAFB (OH): The Department of the Air Force; 2003 Jan. Report No.: CI02-798.
11. Hong YG, Knight D, Kandala R, Candler Gv. Control of normal shock by a single laser pulse. In: *Proceedings of 2nd AIAA flow control conference*; 2004 Jun 28-Jul 1; Portland, Oregon. Reston, VA: AIAA; 2004.
12. Hong YG, Adelgren R, Boguszko M, Elliott G, Knight D. Laser energy deposition in quiescent air. In: *Proceedings of 41st aerospace sciences meeting and exhibit*; 2003 Jan 6–9; Reno, Nevada. Reston, VA: AIAA; 2003.
13. Hong YG, Adelgren R, Elliott G, Knight D, Beutner T. Effect of energy addition on MR→RR transition. *Shock Waves* 2003;**13**(2):113–21.
14. Hong YG, Adelgren R, Elliott G, Knight D, Buetner T, Ivanov M, et al. Laser energy deposition in quiescent air and intersecting shocks. In: *Proceedings of fourth workshop on magneto and plasma aerodynamics for aerospace applications*; 2002 Apr 8–11; IVTAN, Moscow, Russia; 2002.
15. Hong YG, Gaitonde D. Control of edney IV interaction by energy pulse. In: *Proceedings of 44th aerospace sciences meeting and exhibit*; 2006 Jan 9–12; Reno, Nevada. Reston, VA: AIAA; 2006.
16. Kandala R, Candler GV. Numerical studies of laser-induced energy deposition for supersonic flow control. In: *Proceedings of 41st aerospace sciences meeting and exhibit*; 2003 Jan 6–9; Reno, Nevada. Reston, VA: AIAA; 2003.
17. Kandala R, Candler GV. Numerical studies of laser-induced energy deposition for supersonic flow control. *AIAA J* 2004;**42**(11):2266–75.
18. Kandala R, Candler GV. Computational modeling of localized laser energy deposition in quiescent air. In: *Proceedings of 33rd plasmadynamics and lasers conference*; 2002 May 20–23; Maui, Hawai. Reston, VA: AIAA; 2002.
19. Kandala R. Numerical simulations of laser energy deposition for supersonic flow control [dissertation]. Minneapolis(MN): The University of Minnesota. 2005.
20. Sasoh A, Sekiya Y, Sakai T. Supersonic drag reduction with repetitive laser pulses through a blunt body. In: *Proceedings of 40th AIAA plasmadynamics and lasers conference*; 2009 Jun 22–25; San Antonio, Texas. Reston, VA: AIAA; 2009.
21. Kim J-H, Matsuda A, Sakai T, Sasoh A. Drag reduction with high-frequency repetitive side-on laser pulse energy depositions. In: *Proceedings of 40th fluid dynamics conference and exhibit*; 2010 Jun 28-Jul 1; Chicago, Illinois. Reston, VA: AIAA; 2010.
22. Sasoh A, Sekiya Y, Sakai T, Kim J-H, Matsuda A. Wave drag reduction over a blunt nose with repetitive laser energy depositions. *AIAA J* 2010;**48**(12):2811–7.
23. Sasoh A, Sekiya Y, Sakai T, Kim J-H, Matsuda A. Drag reduction of blunt body in a supersonic flow with laser energy depositions. In: *Proceedings of 47th AIAA aerospace sciences meeting including the new horizons forum and aerospace exposition*; 2009 Jan 5–8; Orlando, Florida. Reston, VA: AIAA. 2009.
24. Mori K, Sasoh A. Experiments of laser-pulse-induced drag modulation in supersonic flow. In: *Proceedings of 37th AIAA plasmadynamics and lasers conference*; 2006 Jun 5–8; San Francisco, California. Reston, VA: AIAA; 2006.

Hong Yanji is a researcher in the State Key Laboratory of Laser Propulsion and Application at Equipment Academy. She is mainly focused on investigation of mechanical effects generated by interaction of laser with matters, plasma flow control and optical diagnostics.

Wang Diankai is a doctor of Science and Technology of Weapon. He is a research associate in the State Key Laboratory of Laser Propulsion and Application at Equipment Academy. He is mainly focused on investigation of hypersonic flow control with laser energy.